Title

Novel Nanococktail of a Dual PI3K/mTOR Inhibitor and Cabazitaxel for Castration-Resistant Prostate Cancer

Journal

Advanced Therapeutics, 3(10)

ISSN

2366-3987

Authors

Huang, Yee
Xue, Xiangdong
Li, Xiaocen
et al.

Publication Date

2020-10-01

DOI

10.1002/adtp.202000075

Peer reviewed

HHS Public Access

Author manuscript

Adv Ther (Weinh). Author manuscript; available in PMC 2021 October 01.

Published in final edited form as:

Adv Ther (Weinh). 2020 October ; 3(10): . doi:10.1002/adtp.202000075.

Novel nanococktail of a dual PI3K/mTOR inhibitor and cabazitaxel for castration-resistant prostate cancer

Yee Huang[1], **Xiangdong Xue**[2], **Xiaocen Li**[2], **Bei Jia**[2], **Chong-xian Pan**[3,4], **Yuanpei Li**[2], **Tzu-yin Lin**[3]

[1]Institute of Animal Husbandry and Veterinary Science, Zhejiang Academy of Agricultural Sciences, Hangzhou, Zhejiang 310021, P.R. China

[2]Department of Biochemistry and Molecular Medicine, University of California Davis, Sacramento CA 95817

[3]Department of Internal Medicine, School of Medicine, University of California Davis, Sacramento CA 95817

[4]VA Northern California Health Care System, Mather, CA 95655

Abstract

Prognosis of castration-resistant prostate cancer (CRPC) carries is poor, and no effective therapeutic regimen is yet known. The phosphatidylinositol-3-kinase (PI3K)/protein kinase B (Akt)/mammalian target of rapamycin (mTOR) pathway played a predominant role and may be a promising molecular target for CRPC. However, the toxicity of the dual PI3K inhibitors in clinical trials limits their clinical efficacy for CRPC. To solve this problem, we employed a highly integrated precision nanomedicine strategy to molecularly and physically target CRPC through synergistic effects, enhanced targeted drug delivery efficiency, and reduced unwanted side-effects. Gedatolisib (Ge), a potent inhibitor of PI3K/mTOR, was formulated into our disulfied-crosslinked micelle plateform (NanoGe), which exhibits excellent water solubility, small size (23.25±2 nm), excellent stability with redox stimulus-responsive disintegration, and preferential uptake at tumor sites. NanoGe improved the anti-neoplastic effect of free Ge by 53 times in PC-3M cells and 13 times in C4–2B cells though its enhanced uptake via caveolae- and clathrin-mediated endocytic pathways and the subsequent inhibition of the PI3K/mTOR pathway, resulting in Bax/Bcl-2 dependent apoptosis. In an animal xenograft model, NanoGe showed superior efficacy than free Ge, and synergized with nanoformulated cabazitaxel (NanoCa) as a nanococktail format to achieve a cure rate of 83%. Taken together, our results demonstrate the potency of NanoGe in combination with NanoCa is potent against prostate cancer.

Graphical Abstract

Corresponding Authors: Drs. Yuanpei Li and Tzu-yin Lin, 2700 Stockton Blvd, Sacramento, CA 95817, Phone: 916-7344-420; 916-703-5081, lypli@ucdavis.edu; tylin@ucdavis.edu.

Contributions

YH performed the *in vitro* and *in vivo* experiments. XX did part of the drug loading and TEM experiment. XL synthesized DCM. BJ performed part of the animal experiments. YH, TL, CP and YL designed overall experiments and prepared the manuscripts. All authors commented on the manuscript.

Conflict of interests

Dr. Li holds the patent for DCM and may have interests for commercialization. The authors declare no potential conflicts of interest.

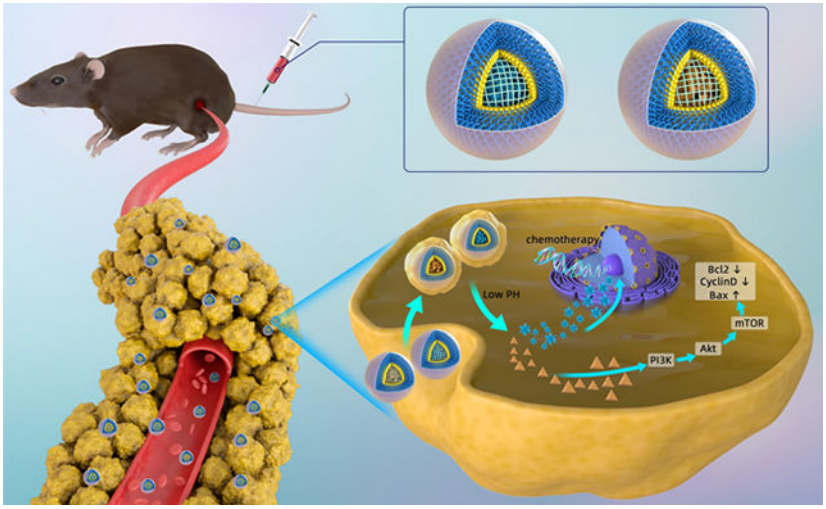

A novel nanococktail of Gedatolisib and Cabazitaxel was developed to improve the therapeutic efficacy against castration-resistant prostate cancer. The nanoformulations were based on disulfide cross-linked micelles, which could significantly increase the water solubility of multiple drug payloads, improve the stability and minimize the premature release of the loaded drug during circulation, preferentially accumulate at tumor sites and release drugs in redox environments.

Keywords

Disulfide cross-linked micelle; Gedatolisib; PI3K pathway; Synergistic antitumor effect

1. Introduction

Prostate cancer is the most frequently diagnosed non-cutaneous malignancy and the second leading cause of cancer-related mortality among men in Europe and the United States. Nearly 30,000 deaths related to prostate cancer are reported per year in the United States.[1–4] Localized prostate cancer is, in general, treated with and sometimes cured with surgery and/or radiation. Patients who present with metastatic or recurrent cancer after local definitive therapy are usually treated with androgen deprivation therapy. Although initial therapy is highly effective, long-term follow-up shows that almost all patients develop castration-resistant prostate cancer (CRPC). Anti-androgen receptor agents such as enzalutamide and apalutamide, androgen synthesis enzyme cytochrome P450 17A1 or CYP17 inhibitor abiraterone, and cytotoxic chemotherapy docetaxel are commonly used under this setting, but only some patients respond to treatment.[5,6] Cabazitaxel is approved by the United States Food and Drug Administration(FDA) for CRPC previously treated with docetaxel but with a response rate of approximately 40%.[7]

Dysregulation of the PI3K/Akt/mTOR pathway is known to contribute to prostate cancer oncogenesis.[8–10] Aberrant activation of this pathway is frequent in prostate cancer cells, mediated through the downregulation in the expression of the tumor suppressor protein, phosphatase and tensin homologue (PTEN).[11] Preclinical and clinical studies have demonstrated the involvement of the PI3K/Akt/mTOR pathway in the regulation of prostate

cancer development. Molecular targeted therapy is an emerging trend to practice precision medicine. Inhibitors of this pathway are thought to achieve clinical benefit in patients with CRPC.[12] Thus, optimizing PI3K inhibitor treatment for CRPC is critical to improve patient outcome. Gedatolisib, a derivative of bis (morpholinotriazine) compounds, is a potent dual PI3K/mTOR inhibitor that has entered clinical trials for treatment of different types of cancers (breast cancer, colorectal cancer, leukemia, endometrial cancer, and lung cancer).[13] However, a phase II study with another dual mTOR inhibitor MLN0128 showed only very limited clinical efficacy due to toxicity related drug reduction.[14] Thus, there is an urgent need to develop more effective yet less toxic regimens for clinical applications.

Application of different combinations of therapeutic agents to improve efficacy and overcome drug resistance is a common clinical practice. Combining the targeting agent gedatolisib with standard cabazitaxel chemotherapy is a reasonable strategy to improve clinical outcome. Cabazitaxel is a novel taxane approved as a second-line therapy for patients with docetaxel-refractory prostate cancer. Cabazitaxel exhibits low affinity for the multidrug resistance transporter, P-glycoprotein, which is known to be active in patients with advanced prostate cancer and taxane-resistant metastatic breast cancer.[15] However, it is also poorly soluble in water and extremely toxic.

Precision medicine involves not only the selection of the correct molecular targeting drugs but also precisely delivering them at target sites. The major hindrance with cabazitaxel and gedatolisib is their low selective distribution and poor water solubility. Drug-induced toxicity remarkably reduces the quality of life in patients. Therefore, we employed a highly integrated precision nanomedicine approach to molecularly and physically target CRPC with our nanococktail platform. Based on our previous work, we newly introduced a disulfide-crosslinked micelle (DCM) system to improve drug solubility (Fig S1), avoid premature release of the loaded drug in the circulation, prolong *in vivo* circulation time, and achieve preferential accumulation at the tumor site via enhanced permeability and retention (EPR) effect.[16] Nano-formulation with excellent tumor-targeting ability may strongly increase therapeutic effects while minimizing unspecific toxicity and side-effects.[17,18]

We integrated two major concepts to establish future precision medicine in CRPC management to achieve better efficacy with decreased toxicity via molecular and physical targeting approaches. The first one aims to combine a molecular targeting agent with a second-line chemotherapy, and the other approach involves formulation of a nanococktail strategy to enhance tumor-targeted drug delivery using nanotechnology. Instead of co-loading two drugs, the nanococktail strategy provides the flexibility of adjusting drug administration regimen as per the clinical need. Herein, we first characterized nanoformulated gedatolisib (NanoGe) and confirmed its superior anti-CRPC effect both *in vitro* and *in vivo*. Later, using an animal model we show that NanoGe synergized with NanoCa to achieve a cure rate of 83% and an acceptable toxicity profile. The combination was more effective in inhibiting the PI3K/Akt/mTOR pathway by increasing bcl-2-dependent apoptosis. These results lay a strong foundation for future clinical translation and may impact the management of patients with CRPC.

2. Materials and methods

2.1. Preparation of nanoformulated gedatolisib and cabazitaxel

PEG5k-Cys4-L8-CA8 polymers were synthesized as previously described.[16] Gedatolisib (10mM) was mixed with PEG5k-Cys4-L8-CA8 telodendrimers (20 mg) and dissolved in chloroform (1 mL). This organic solution was evaporated using a Heidolph rotary evaporator (Elk Grove Village, IL, USA) to obtain a thin film, which was hydrated with water and sonicated for 20 min (ColeeParmer sonicator, Vernon Hills, IL, USA). The resulting drug-loaded micelles were cross-linked via O_2-mediated oxidation as previously described.[16] Nanoformulated cabazitaxel was prepared in the same manner and mixed with NanoGe at a 1:1 (v/v) ratio and sonicated for 10 min to obtain a homogeneous system.

Loading efficiency was spectrophotometrically analyzed using a microplate reader (SpectraMax M3, Molecular Devices, Sunnyvale, CA, USA) after releasing the drug from micelles by adding DMSO (90%, v/v) and sonicating for 10 min. DCMs mixed with DMSO (1:4, v/v) were used as a blank control. Drug loading was determined using a standard curve generated from a series of gedatolisib/DMSO standard solutions.

To visualize cellular uptake and *in vivo* biodistribution of DCMs, the hydrophobic near-infrared fluorescence (NIRF) dye DiD (0.5 mg/mL) was coloaded with gedatolisib into DCMs, as described above. The micelle solution was sterilized using a 0.22 mM filter.

2.2 Physicochemical characterization and stability testing of NanoGe

The morphology and particle size distribution of NanoGe were analyzed by transmission electron microscopy (TEM, Philips CM-120, Amsterdam, Netherland) and a dynamic light scattering (DLS) instrument (Microtrac, San Diego, CA, USA), respectively. Gedatolisib concentration of NanoGe was maintained at 10 mM during measurements.

The stability of NanoGe was analyzed by monitoring its particle size distribution by DLS at predetermined time intervals.

The *in vitro* drug release profile of NanoGe was measured using the dialysis method.[19] Aliquots of NanoGe (Ge loading in DCM was 1 mM) were injected into dialysis cartridges with a molecular-weight cutoff (MWCO) of 3.5 kDa (Thermo Fisher Scientific, Waltham, MA, USA). Cartridges were dialyzed against 1 L of PBS (or 20 mM GSH) at 37 ^{o}C by shaking at 80 rpm (Radnor shaker, VWR, PA, USA). The concentration of Ge remaining in the dialysis cartridge at various time points was measured by absorbance spectrophotometry at 320 nm. For comparison, the release profile of Ge (1 mM, in DMSO) was determined under the same conditions.

2.3 Cell viability assay

PC-3M and C4–2B cell lines were purchased from the American Type Culture Collection (ATCC, Manassas, VA, USA) and cultured in RPMI-1640 medium supplanted with 10% (v/v) fetal bovine serum and 0.5% penicillin/streptomycin at 37 ^{o}C.

The effect of NanoGe on the cell viability was determined by MTS assay (Promega), as previously described.[20] Briefly, PC-3M and C4–2B cells were seeded in 96-well plates and treated with different concentrations of NanoGe, Ge (ranging from 10^{-4} μM to 10 μM) and DCM, NanoCa, or NanoCaGe as indicated. MTS assay was performed to assess cell viability after 48 h of treatment. Absorbance at 490 nm was measured using a plate reader. Cell viability percentage was calculated by measuring the percentage of viable cells in treatment group as compared to that in untreated controls.

2.4 Cellular uptake and subcellular distribution

PC-3M cells were seeded in 8-well tissue culture chamber slides (BD Biosciences, San Jose, CA) at a density of 10,000 cells/well. After attachment, cells were treated with DiD-labeled NanoGe (500 μg/mL DiD and 1 μM Ge) for 4 h, washed twice with PBS, and fixed with 4% paraformaldehyde. Nuclei were stained with Hoechst 33342 (Thermo Fisher) for 5 min. To determine subcellular distribution, LysoTracker (Invitrogen) was used to stain lysosomes after treatment of cells with DiD-labeled NanoGe for 4 h. Slides were observed under a confocal laser scanning microscope (Carl Zeiss). To study quantitative and dynamic changes during the cellular uptake of DiD-labeled NanoGe at 1, 2, 3, and 4 h, flow cytometry (BD FACSCanto™, USA) was used.

2.5 Apoptosis detection and cell cycle analysis

PC-3M cells were seeded in a 6-well plate at a density of 60,000 cells/ well. After 24 h, these cells were exposed to different concentrations of NanoGe and gedatolisib for 24 h. Early and late apoptosis were assessed by Annexin V-FITC/PI dual staining as previously described (Biolegend, San Diego, CA).[21] For cell cycle analysis, the cells were harvested after different treatments and fixed with cold 70% ethanol at 4°C for overnight. Cells were then incubated with 20 μg/mL of RNase A and 25 μg/mL PI for 30 min in the dark. Samples were analyzed by BD FACSCanto™ cell analyzer.

2.6 Western blot analysis

Several proteins involved in cell signaling, apoptosis, and cell cycle regulation were analyzed by western blotting. Total cellular protein was extracted from PC-3M cells following homogenization with RIPA buffer (Cell Signaling Technology) after 6 h treatment with free Ge, NanoGe, NanoCa, or NanoCaGe. 50 μg of total protein lysate was subjected to sodium dodecyl sulfate-polyacrylamide gel electrophoresis (SDS-PAGEs), and the separated protein bands were transferred onto nitrocellulose membranes. The membranes were incubated with appropriate antibodies and then probed with horseradish peroxidase (HRP)-conjugated secondary antibodies. Signals were visualized by Amersham ECL Plus Western Blotting Detection System (Amersham, GE Healthcare, Little Chalfont, Buckinghamshire, UK) under an imaging system (Bio-Rad) and data were quantified by ImageJ. The following primary antibodies were used: p-PI3K, mTOR, p-mTOR, p-Akt, Akt, Bcl-2, Bax, cyclin D1, p-cyclin D1, and glyceraldehyde 3-phosphate dehydrogenase (GAPDH) (Cell Signaling Technology, Danvers, MA, USA).

2.7 Prostate cancer xenograft mouse model for near-infrared red fluorescence (NIRF) imaging

All animal experiments were performed in accordance with the guidelines approved by the Animal Care and Use Committee of the UC Davis. PC-3M cells were subcutaneously injected into nude mice on both sides of their flanks (The Jackson Laboratory, Sacramento, CA). Once the prostate cancer xenograft mouse model was established, mice were intravenously administrated with DiD-labeled NanoGe (2.5 mg/kg DiD and 10 mg/kg Ge) and whole body imaging was acquired at indicated time points. At 24 h time-point, animals were sacrificed and tumors and other major organs were harvested for *ex vivo* imaging.

2.8 *In vivo* anti-cancer efficacy study in prostate cancer xenograft model

Nude mice (The Jackson Laboratory, Sacramento, CA) were subcutaneously injected with PC-3M cells (5×10^6 cells/mice). Once the tumors reached the size of 100–150 mm^3, mice were divided into 8 groups (6 mice/group) as follows: PBS (Control), gedatolisib (10mg/kg), gedatolisib (20mg/kg), empty DCM, NanoGe (10mg/kg Ge), NanoGe (20mg/kg Ge), NanoCa (10mg/kg Ca), NanoGeCa (10mg/kg Ge & 10mg/kg Ca). Mice received drugs via tail-vein injection every 3 days for a total of 5 doses. Body weights and tumors were measured every 4 days, and tumor volume was calculated based on the formula: length × ($width^2$) /2.

2.9 Statistical analysis

All quantitative measurements are presented as mean ± standard error (SE), and statistical analyses were performed using GraphPad Prism (GraphPad Software, CA, USA). One-way analysis of variance (ANOVA) followed by Tukey's test was used for comparing multi-group data. The level of significance was labeled by *, **, and *** corresponding to a P value < 0.05, < 0.01, and < 0.001, respectively.

3 Results

3.1 Characterization and stability of gedatolisib-loaded disulfide-crosslinked micelles

We have previously described the formulation of self-assembling disulfide-crosslinked micelles (Fig S1)to avoid premature release of the loaded cargo during circulation.[16] Based on our previous work, here we loaded DCM with Ge (Fig. 1A) at an average loading efficiency of 94.6% ± 0.3%. NanoGe, as observed with TEM, were spherical in shape and had a uniform size (Fig. 1B) of 23.25 ± 2 nm, as measured by DLS (Fig. 1C). NanoGe showed excellent stability at 4 °C; both the average particle size and PDI showed slightly increased over 60 days (Fig. 1D).

The drug release profile of Ge from NanoGe was monitored by the dialysis method. Within 100 h, about 58% Ge was released from DCMs. However, in the presence of the reducing agent GSH (at its intracellular level, 10 mM), Ge release increased (Fig. 1E). The intracellular concentration of GSH (10 mM) is substantially higher than its extracellular level (2 mM).[22] The redox-responsive dissociation of the cross-link inside DCMs facilitated the drug release.[16] Therefore, once NanoGe accumulated inside cancer cells, the intracellular reductive GSH could effectively induce drug release.

3.2 DCM delivered gedatolisib within the cells through an endocytic pathway

To investigate the cellular uptake of NanoGe, we labeled NanoGe with DiD and studied its uptake using confocal microscopy. After 2 h incubation, NanoGe mainly aggregated inside PC-3M cells, while some particles adhered onto the plasma membrane (Fig. 2A).

To investigate the internalization route of the DCMs, we stained lysosomes with LysoTracker® Green. The intracellular fluorescence pattern of red-labeled NanoGe was colocalized with the cell lysosomes (green) (Fig. 2B). Thus, DCM delivered Ge into the cancer cells via the endocytic pathway.

To demonstrate the internalization of NanoGe into cells via endocytic pathway, various endocytosis inhibitors were used. Genistein, an endocytotic inhibitor of caveolae-mediated endocytosis, significantly inhibited the cytotoxicity of NanoGe against prostate cancer cells. Chlorpromazine, an endocytotic inhibitor of clathrin-mediated endocytosis, also significant suppressed the cytotoxic effects of NanoGe (Fig. 2C). Other inhibitors such as Cytochalasin D, an endocytotic inhibitor of macropinocytosis-mediated endocytosis, showed no effect on the action of NanoGe (data not shown). These results indicated that caveolae- and clathrin-mediated endocytotic pathway were the main mechanisms underlying the cellular uptake of NanoGe.

3.3 Gedatolisib-loaded DCM exhibited enhanced cytotoxicity against prostate cancer cells and induced apoptosis and cell cycle arrest

The *in vitro* cytotoxicity effect of NanoGe was compared to that of free Ge and DCM in two prostate cancer cell lines (PC-3M and C4–2B). PC-3 cell line was derived from a 62-year-old white man with lumbar vertebral metastasis. PC-3M cell line was established from a PC-3 xenograft and is more aggressive than the parental xenograft.[23] C4–2B is a bone metastatic subline of C4–2, which was derived from LNCaP and could metastasize to lymph nodes and bone tissue.[24]

As shown in Fig. 3A, NanoGe significantly improved the cytotoxicity of Ge in both cell lines. The IC50 value of Ge was about 53 and 13 times higher than that of NanoGe in PC-3M and C4–2B cells, respectively.

The pro-apoptotic effects of NanoGe were examined in these cell lines by flow cytometry. NanoGe significantly increased the population of cells undergoing apoptosis (Annexin V-positive cells) as compared with Ge at the same concentration. NanoGe also induced apoptosis in a dose-dependent manner (Fig. 3B, Fig. S2, and Fig. S3).

The effect of NanoGe on cell cycle progression was evaluated by flow cytometric analysis after 24 h treatment. Ge-treated cells showed higher G1 cell population with a concomitant decrease in G2 population in a dose-dependent manner as compared with control cells. In the cells treated with Ge-loaded DCMs, the G1 arrest effect was further enhanced (Fig. 3C).

3.4 NanoGe enhanced the inhibition of the PI3K/mTOR pathway in prostate cancer cells

The mechanism underlying the antitumor activity of NanoGe was investigated. As gedatolisib is a potent PI3K/mTOR inhibitor, we evaluated the effects of NanoGe and

gedatolisib on the phosphorylation of PI3K and mTOR by western blot analysis. While gedatolisib decreased p-PI3K, p-mTOR, and mTOR protein levels, this effect was more pronounced by NanoGe treatment (Fig. 4A and 4C).

The level of the anti-apoptotic protein Bcl-2 decreased after Ge treatment. Compared with Ge, NanoGe induced a further decrease in Bcl-2 expression level. While Ge treatment increased the expression of the pro-apoptotic protein, Bax, the level of Bax was further increased following NanoGe treatment (Fig. 4B and 4C). The expression of the proteins involved in the cell cycle regulation was also investigated by western blotting. As shown in Fig. 4B and 4C, Ge and NanoGe treatment both induced a dose-dependent decrease in the protein levels of cyclin D and p-cyclin D; this effect was more pronounced by NanoGe.

3.5 *In vivo* NanoGe was preferentially delivered at the tumor site

To investigate whether NanoGe could passively target tumor sites via the EPR effect, noninvasive NIRF optical imaging was performed to monitor the biodistribution of DiD-labeled NanoGe in a xenograft tumor model. DiD is an NIRF dye that allows deep tissue imaging, given its high penetration ability and low tissue absorption and scattering. We found that DiD-labeled NanoGe preferentially accumulated at the tumor site. A significant contrast in fluorescence signal was observed between tumor and background at 24 h after administration that sustained up to 72 h (Fig. 5A). *Ex vivo* imaging at 72 h post-injection further confirmed the preferential uptake of NanoGe at the tumor site as compared to that in normal organs (Fig. 5B). Quantitative data also showed that the mean fluorescence of tumor was significantly higher than that of other organs (Fig. 5C). The spleen and liver had higher mean fluorescence than the other organs evaluated.

3.6 *In vivo* NanoGe exhibited a better therapeutic efficacy in a PC-3M xenograft tumor model

We established a PC-3M xenograft tumor model to investigate the therapeutic effects of NanoGe. PC-3M tumor-bearing mice were intravenously administered with PBS (control), gedatolisib (10 and 20 mg/kg), DCM, or NanoGe (10 and 20 mg/kg). A total of five doses were administered every 3 days (day 0, 3, 6, 9, and 12). We found that NanoGe delayed the progression of tumor growth as compared with free gedatolisib at same dose (Fig. 5C). Further, NanoGe also prolonged the survival time of mice as compared to free gedatolisib; the median survival times for NanoGe and free gedatolisib were of 36 (20mg/kg NanoGe) and 38 (10mg/kg NanoGe) days versus 30 (20mg/kg Ge) and 32 (10mg/kg Ge) days, respectively (Fig. 5D).

The potential toxicity associated with treatment was assessed by measuring body weight. The mice receiving NanoGe (20 mg/kg) showed a slight transient decrease in body weights during the treatment cycle as compared with the mice from PBS and DCM groups, but eventually their body weights rapidly recovered (Fig. 5E).

3.7 *In vivo* NanoCaGe exhibited synergistic cytotoxicity and excellent anti-tumor effect

For the better inhibition of tumor progression, we further employed a drug combination to enhance the therapeutic efficiency against prostate cancer. PI3K inhibitor nanoformulation

(NanoGe) was combined with cabazitaxel-loaded DCM (NanoCa). Cabazitaxel is a taxane used in combination with prednisone or prednisolone for the treatment of patients with metastatic hormone-refractory prostate cancer.[25] In 2010, cabazitaxel has been approved by the FDA to treat CRPC. The loading efficiency of NanoCa was 89% ± 0.78%. Its particle size was around 20 nm and PDI was 0.128. NanoCa showed excellent stability (Fig. S4).

The cytotoxicity effects of NanoGe (10^{-4} μM Ge) in combination with different concentrations of NanoCa were analyzed using the MTS assay. As shown in Fig. 6A, NanoGe and NanoCa combination therapy was more effective in killing the PC-3M cells over single NanoGe and NanoCa treatment. As shown in Fig. 6B, the combination index (CI) of all concentrations showed strong synergistic effects (CI < 0.3 indicates strong synergy).

We investigated the mechanism underlying the anti-neoplastic activity of NanoCaGe. Changes in protein levels after treatment with NanoCaGe were also compared with those observed after single NanoGe or NanoCa treatment. As shown in Fig. 6C, the expression of p-Akt, p-cyclin D, cyclin D, Bcl-2 significantly decreased following NanoCaGe treatment as compared with that observed after single nanoformulation treatment. The level of the pro-apoptotic protein Bax significantly increased in the combination group.

The *in vivo* antitumor efficacy of NanoCaGe was investigated and compared with that of NanoGe and NanoCa alone in the xenograft tumor model. The results showed that NanoGe (10 mg/kg) in combination with NanoCa (10 mg/kg) could significantly inhibit tumor growth and exert best therapeutic efficacy (Fig. 6D). In NanoGe group, one mouse died on day 36; hence, we stopped monitoring average tumor size for all three groups. On day 40, 5 out of 6 mice (83.33%) were cured with no visible tumors. By day 60, the survial rate of NanoCaGe was 100%, while that of NanoGe was 0 and NanoCa was 25% (Fig. 6E).

The potential toxicity associated with treatment was assessed by measuring changes in body weight. Body weight loss was slightly more in the mice receiving NanoCa (10 mg/kg) and NanoCaGe (10 mg/kg of each of cabazitaxel and gedatolisib) during treatment cycle, but body weights of these mice recovered and were normal thereafter (Fig. 6F). The results on day 4 from the last dosage showed that serum markers (ALT, AST, total bilirubin, BUN and creatinine) in all DCM formulation groups were within the normal range, indicative of the absence of any hepatic and renal toxicities. CBC results showed that WBC, Lymphocyte, Monocyte, Eosinophil, Basophil, RBC, Hemoglobin, Hematocrit, Mean Corpuscular Volume(MCV), Mean Corpuscular Hemoglobin(MCH), Mean Corpuscular Hemoglobin Concentration(MCHC), red cell distribution width (RDW), mean platelet volume(MPV) of the mice in all the DCM formulation groups were within the normal range, except that NanoCa and the combination group showed higher level platelets counts (Tables 1 and 2). The results excluded the potential hematologic toxicity associated with DCM formulation.

4 Discussion

Most advanced prostate cancers are characterized with the upregulation in the PI3K/Akt pathway, which controls diverse cellular processes, including cell proliferation, growth,

survival, protein synthesis, and glucose metabolism.[26–29] Activation of the PI3K/Akt pathway in prostate cancer is often associated with the functional loss of the tumor suppressor phosphatase and tensin homolog(PTEN) located on chromosome 10, resulting in the dephosphorylation of PI3K substrates or mutations in the PI3K itself.[30,31] Many pharmaceutical companies and academic institutions are attempting to develop small molecule inhibitors to specifically target PI3K/mTOR, a promising targeted therapy for advanced prostate cancer.[26,32–34] However, recent clinical trial revealed disappointment of PI3K inhibitor results due to toxicity related dose reduction.[14] We employed two different approaches to address this challenge as follows: to combine standard chemotherapeutic drugs to achieve synergistic effects and to improve targeted delivery while decreasing unwanted toxicity and increasing efficacy.

Clinical trials have revealed only modest anti-tumor efficacy of PI3K inhibitors in prostate cancer, suggesting that monotherapy may not be very effective for solid tumors.[35] The combination of PI3K inhibitors and other agents is thought to exert stronger antitumor effects, but the associated side-effects prevent the translation of basic research results into preclinical and clinical models.[36] Cabazitaxel is one of the second line chemotherapeutic agents, which belongs to anti-microtubular class chemo-drug. It inhibits microtubule disassembly and induces cell apoptosis.[37–39] It was only moderately effective at a response rate of 40%, but exhibited highly toxicity, as over 80% patients developed severe (Grade 3) or life-threatening (Grade 4) toxicities.[40]

The common obstacles in drug development are poor water solubility, poor bioavilability, and non-specific distribution-related toxicity of drugs. The cross-linked micelles exhibited preferential tumor targeting as compared with non-cross-linked micelles and exhibited better drug-loading efficiency, enhanced stability, and prolonged *in vivo* circulation time.[16] Both gedatolisib and cabazitaxel were administered as nano-formulations and their synergistic therapeutic effects elicited were investigated. This is the first study to use the combination of two micelle formulations for the targeted therapy of CRPC.

The disulfide bonds inside DCM are reversible and may be reduced by GSH, a thiol-containing tripeptide generated in the cell cytoplasm. GSH level is high in many human and murine tumor cells, thereby facilitating disulfide bond reduction and drug release.[41,42] This specific phenomenon, therefore, facilitates the intracellular release of the encapsulated drug taken up via caveolae- and clathrin-mediated endocytotic pathways (Fig. 2C and 3A), resulting in enhanced cytotoxicity. NanoGe significantly inhibited the expression of proteins related to the PI3K pathway (Fig. 4). Furthermore, NanoGe exerted apoptotic effects and mediated cell cycle arrest through the PI3K/Akt/mTOR pathway (Fig. 3B and 3C).

According to our previous research, small micelles showed tumor delivery and penetration than large ones.[43,44] NanoGe had small in diameter (23.25±2 nm) and good stability and was highly water-soluble. NanoGe was internalized into tumor cells through caveolae- and clathrin-mediated endocytotic pathways (Fig. 2B). Given the size-mediated EPR effect, NanoGe preferentially accumulated at the tumor site and its uptake in other normal organs such as the skin and muscle was low, as revealed by NIRF optical imaging (Fig. 5A and 5B).

Hence, higher amount of Ge could penetrate into the tumor, resulting in superior tumor growth inhibition.

To improve drug-targeting ability and reduce systemic toxicity, nanodelivery systems and target molecular therapy agents are gaining attention.[45–48] To date, very few nanomedicines have been approved for clinical use, including albumin-bound paclitaxel, polymeric micelle-formulated paclitaxel, and non-PEGylated liposomal doxorubicin.[49]

In the present study, we employed DCM as the targeting delivery system and separately loaded it with a chemodrug (Ca) and a small molecular inhibitor (Ge). Both NanoGe and NanoCa showed excellent stability. The combination therapy exhibited a strong synergistic effect by controlling tumor growth both *in vitro* and *in vivo*. *In vitro*, the CI value was analyzed using CompuSyn software 1.0. All CI values were lower than 0.3, indicating a strong synergism between NanoGe and NanoCa. Further, the combination therapy effectively reduced drug dose and toxicity. *In vivo*, NanoGe (20 mg/kg) was more effective than NanoGe (10 mg/kg) in controlling tumor growth but was more toxic, as evident from the decrease in the body weight and survival rate of mice. The combination of NanoGe (10 mg/kg) and NanoCa (10 mg/kg) was the most efficacious regimen in terms of tumor growth inhibition and survival time as compared to single formulation regimens. NanoGe effectively inhibited the PI3K/Akt/mTOR pathway. Mechanistic studies showed that the combined nanococktail was more efficacious in inhibiting antiapoptotic (Bcl-2) and cell cycle-related (cyclin D1) proteins while increasing the expression of the pro-apoptotic protein Bax.

Our study demonstrated the potency of NanoGe to inhibit PI3K/mTOR and exert antiproliferative effects in prostate cancer cells. Several molecular pathways were involved underlying the cytotoxic mechanism of action of NanoGe, including induction of apoptosis via the PI3K/Akt/mTOR pathway and G1 cell cycle arrest. NanoGe showed high loading capacity, optimal particle size, outstanding stability, sensitive redox response, and sustained drug release profiles. NIRF labeling of NanoGe revealed its preferential uptake and superior antitumor efficacy in prostate cancer xenograft model. Furthermore, the combination of NanoGe and NanoCa exhibited synergistic antitumor activities. In conclusion, NanoCaGe nanococktail could be potentially applicable for the targeted delivery of chemotherapeutic agents and small molecular inhibitors. It may enhance the therapeutic effects in the management for CRPC. These findings also support the potential impact of integrated precision nanomedicine strategy in the clinical management of different types of cancers.

Supplementary Material

Refer to Web version on PubMed Central for supplementary material.

Acknowledgments

We thank the financial support from NIH/NCI (R01CA199668, 1R01CA232845), NIH/NICHD (R01HD086195), ACS IRG (95-125-13), K12 (5K12CA138464-08, PI: Dr. Lara), UC Davis Comprehensive Cancer Center Support Grant (CCSG) awarded by the National Cancer Institute (NCI P30CA093373), China Agricultural Research System (No. nycytx-44-3-2), and Merit Review (Award # I01 BX001784, 1I01BX003840-01 and 1R01CA176803-01), and The contents do not represent the views of the U.S. Department of Veterans Affairs or the United States Government.

References

[1]. Jemal A, 2010 CA-Cancer J Clin 2011, 60(2), 277–300.

[2]. Siegel R, Ma JM, Zou ZH, Jemal A, CA-Cancer J Clin 2014, 64(1), 9–29. [PubMed: 24399786]

[3]. Siegel RL, Miller KD, Jemal A, CA-Cancer J Clin 2015, 65(1), 5–29. [PubMed: 25559415]

[4]. Liu Y, Hegde P, Zhang F, Hampton G, Jia S, Front. Endocrinol. (Lausanne) 2012, 3, 72. [PubMed: 22661971]

[5]. Renna M, Front. Pharmacol. 2016, 7, 431. [PubMed: 27920721]

[6]. Wang H, Cai S, Bailey BJ, Saadatzadeh MR, Ding J, Tonsing-Carter E, Georgiadis TM, Zachary GT, Long EC, Minto RE, Gordon KR, Sen SE, Cai W, Eitel JA, Waning DL, Bringman LR, Wells CD, Murray ME, Sarkaria JN, Gelbert LM, Jones DR, Cohen-Gadol AA, Mayo LD, Shannon HE, Pollok KE, J. Neurosurg. 2017, 126(2), 446–59. [PubMed: 27177180]

[7]. Onstenk W, Sieuwerts AM, Kraan J, Van M, Nieuweboer AJ, Mathijssen RH, Hamberg Paul P, Meulenbeld HJ, De LB, Dirix LY, Soest RJ, Lolkema MP, Martens JW, Weerden WM, Jenster GW, Foekens JA, Wit R, Sleijfer S, Eur. Urol. 2015, 68(6), 939–45. [PubMed: 26188394]

[8]. Claudio F, Clin. Cancer Drugs 2016, 3, 36–62.

[9]. Wise HM, Hermida MA, Leslie NR, Clin. Sci. (Lond) 2017, 131(3), 197–210. [PubMed: 28057891]

[10]. Edlind MP, Hsie AC, Asian J Androl. 2014, 16(3), 378–86.

[11]. Morgan TM, Koreckij TD, Corey E, Curr. Cancer Drug Targets 2009, 2(9), 237–49.

[12]. Yan G, Ru Y, Wu K, Yan FQ, Wang QH, Wang JX, Pan T, Zhang M, Han H, Li X, Zou L, Prostate 2017, 78, 166–77. [PubMed: 29181846]

[13]. Studies on Gedatolisib http://clinicaltrials.gov/.

[14]. Graham L, Banda K, Torres A, Carver BS, Chen Y, Pisano K, Shelkey G, Curley T, Scher HI, Lotan TL, Hsieh AC, Rathkopf DE, Invest. new drugs 2018, 36(3), 458–67. [PubMed: 29508246]

[15]. Duran GE, Derdau V, Weitz D, Philippe N, Blankenstein J, Atzrodt J, Sémiond D, Gianolio DA, Macé S, Sikic BI, Cancer Chemother. Pharmacol. 2018, 81(6), 1095–1103. [PubMed: 29675746]

[16]. Li Y, Xiao K, Luo J, Xiao W, Lee JS, Gonik AM, Dong TA, Lam KS, Biomaterials 2011, 32(27), 6633–45. [PubMed: 21658763]

[17]. Li S, Deng Q, Li X, Huang Y, Li X, Liu F, Wang H, Qing W, Liu Z, Lee C, Biomaterials 2019, 216, 119252. [PubMed: 31212086]

[18]. Xue X, Huang Y, Bo R, Jia B, Wu H, Yuan Y, Wang Z, Ma Z, Ding D, Xu X, Yu W, Lin T, Li Y, Nat. Commun. 2018, 9(1), 3653. [PubMed: 30194413]

[19]. Xiao K, Luo J, Fowler WL, Li Y, Lee JS, Xing L, Cheng RH, Wang L, Lam KS, Biomaterials 2009, 30(30), 6006–16. [PubMed: 19660809]

[20]. Xiao K, Luo JT, Li Y, Lee JS, Fung G, Lam KS, Control J. Release 2011, 155(2), 272–81.

[21]. Long Q, Lin T, Huang Y, Li X, Ma A, Zhang H, Carney R, Airhart S, Lam KS, deVere White RW, Pan C, Li Y, Nanomed-Nanotechnol. 2018, 14, 789–99.

[22]. Li Y, Zhu L, Liu Z, Cheng R, Meng F, Cui J, Ji S, Zhong Z, Angew Chem-Int. Edit 2009, 48(52), 9914–18.

[23]. Sobe RE, Sadar MD. J. Urol. 2005, 173(2), 360–72. [PubMed: 15643173]

[24]. Liu A, Brubaker KD, Goo YA, Quinn JE, Karl S, Sorensen CM, Vessella RL, Belldegrun AS, Hood LE, Prostate 2004, 60(2), 98–108. [PubMed: 15162376]

[25]. Chen W, Xu X, Jia H, Lei Q, Luo G, Cheng S, Zhou R, Zhang X, Biomaterials 2013, 34(34), 8798–807. [PubMed: 23932289]

[26]. Choo GS, Lee HN, Shin SA, Kim HJ, Jung JY, Mar. Drugs 2016, 14(7), 126.

[27]. Xia P, Xu X, Am. J. Cancer Res. 2015, 5(5), 1602–1609. [PubMed: 26175931]

[28]. Manning BD, Cantley LC, Cell 2007, 129(7), 1261–74. [PubMed: 17604717]

[29]. Engelman JA, Luo J, Cantley LC. Nat. Rev. Genet. 2006, 7(8), 606–19. [PubMed: 16847462]

[30]. Talesa VN, Ferri I, Bellezza G, Love HD, Sidoni A, Antognelli C. Prostate 2017, 77(2), 196–210. [PubMed: 27696457]

[31]. Wozniak DJ, Kajdacsy-Balla A, Macias V, Ball-Kell S, Zenner ML, Bie W, Tyner AL, Nat. Commun. 2017, 8(1), 1508. [PubMed: 29142193]

[32]. Janku F, Yap YA, Meric-Bernstam F, Nat. Rev. Clin. Oncol. 2018, 15(5), 273–291. [PubMed: 29508857]

[33]. Kaarbo M, Mikkelsen OL, Malerod L, Qu S, Lobert VH, Akgul G, Cell Oncol. 2010, 32(1–2), 11–27. [PubMed: 20203370]

[34]. Polivka J, Janku F, Pharmacol. Ther. 2014, 142(2), 164–75. [PubMed: 24333502]

[35]. Martelli AM, Chiarini F, Evangelisti C, Cappellini A, Buontempo F, Bressanin D, Fini M, McCubrey JA, Oncotarget 2012, 3, 371–394. [PubMed: 22564882]

[36]. Daniele B, Sazzad H, Young AC, Anabel F, Yelena K, Dana Y, Pullikuth A, Sui G, Sadelain M, Debinski W, Kulik G, Neoplasia 2013, 15(10), 1172–83. [PubMed: 24204196]

[37]. Karami H, Baradaran B, Esfahani A, Estiar MA, Naghavi-Behzad M, Sakhinia M, Sakhinia E, Asian Pac. J. Cancer P 2013, 14(12), 7719–24.

[38]. Horton SJ, Huntly BJ, Haematologica 2012, 97(7), 966–74. [PubMed: 22511496]

[39]. Gardin C, Chevret S, Pautas C, Turlure P, Raffoux E, Thomas X, Quesnel B, de Revel T, de Botton S, Gachard N, Renneville A, Boissel N, Preudhomme C, Terré C, Fenaux P, Bordessoule D, Celli-Lebras K, Castaigne S, Dombret H, J. Clin. Oncol. 2013, 31(3), 321–7. [PubMed: 23248249]

[40]. Hugo W, Zaretsky JM, Sun L, Song C, Moreno BH, Hu-Lieskovan S, Berent-Maoz B, Pang J, Chmielowski B, Cherry G, Seja E, Lomeli S, Kong X, Kelley MC, Sosman JA, Johnson DB, Ribas A, Lo RS, Cell 2016, 165(1), 35–44. [PubMed: 26997480]

[41]. Black SM, Wolf CR, Pharmacol. Ther. 1991, 51(1), 139–54. [PubMed: 1685247]

[42]. Kartalou M, Essigmann JM, Mutat. Res. 2001, 478(1–2), 23–43. [PubMed: 11406167]

[43]. Li Y, Xiao K, Luo J, Lee J, Pan S, Lam KS, Control J. Release 2010, 144(3), 314–23.

[44]. Luo J, Xiao K, Li Y, Lee J, Shi L, Tan Y, Xing L, Holland CR, Liu GY, Lam KS, Bioconjug. Chem. 2010, 21(7), 1216–24. [PubMed: 20536174]

[45]. Kang H, Hu S, Cho MH, Hong SH, Choi Y, Choi H, Nano Today 2018, 23, 59–72. [PubMed: 31186672]

[46]. Patil Y, Shmeeda H, Amitay Y, Ohana P, Kumar S, Gabizon A, Nanomedicine 2018, 14(4), 1407–1416. [PubMed: 29680672]

[47]. Cherian AM, Nair SV, Lakshmanan VK, J. Nanosci. Nanotechno. 2014, 14(1), 841–852.

[48]. Sanna V, Sechi M. Nanomedicine 2012, 8 Suppl 1: S31–6. [PubMed: 22640911]

[49]. Wang X, Kong D, Lin Y, Li X, Izumiya Y, Ding X, Zhang L, Hu X, Yang J, Gao S, Lam KS, Li Y, Acta Pharmacol. Sin. 2017, 38(6), 931–42. [PubMed: 28552907]

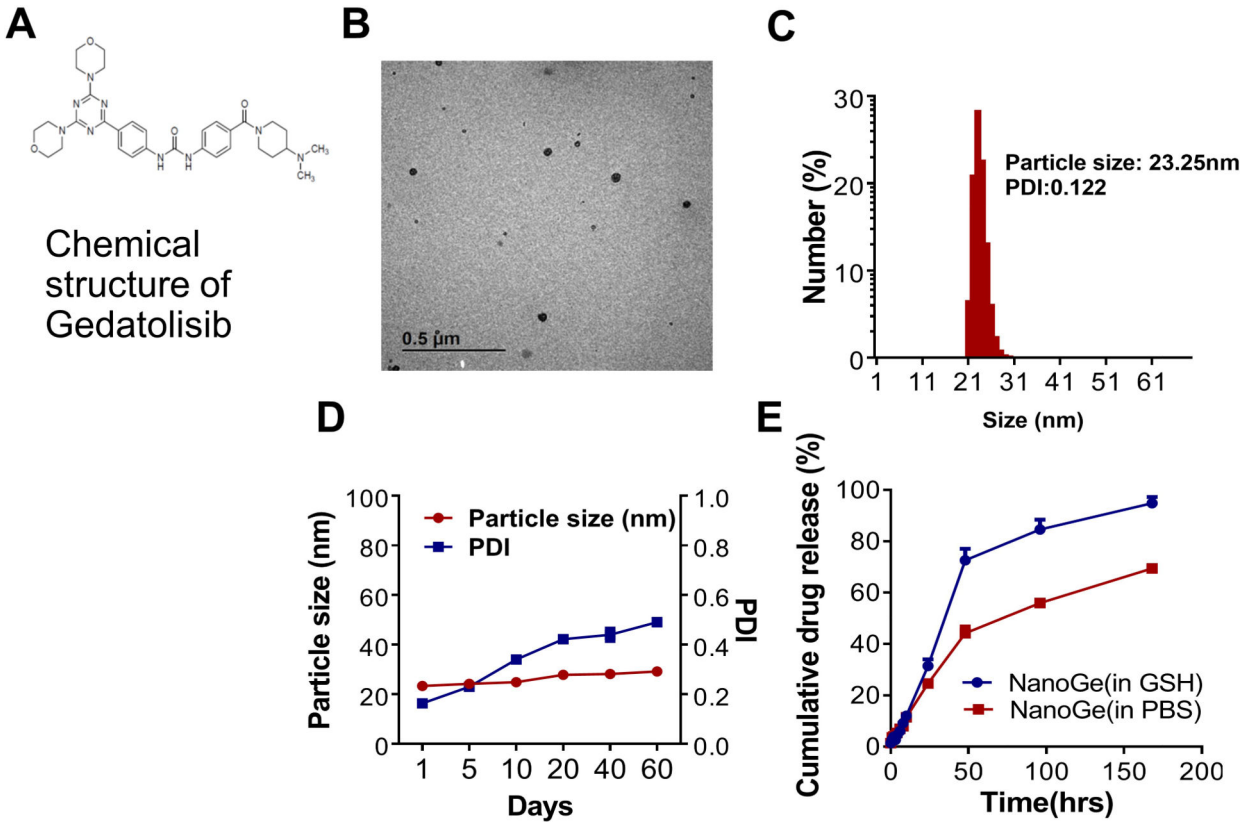

Fig 1.

Characterization of gedatolisib loaded disulfide cross-linked micelles (NanoGe). (A) The chemical structure of gedatolisib. (B) Morphology of NanoGe was analyzed by TEM. (C) Size distribution of NanoGe was analyzed by DLS. (D) Stability of NanoGe was evaluated by monitoring the particle size and PDI value by DLS at predetermined time intervals. (E) The release profile of NanoGe within 168 hours was measured by dialysis method.

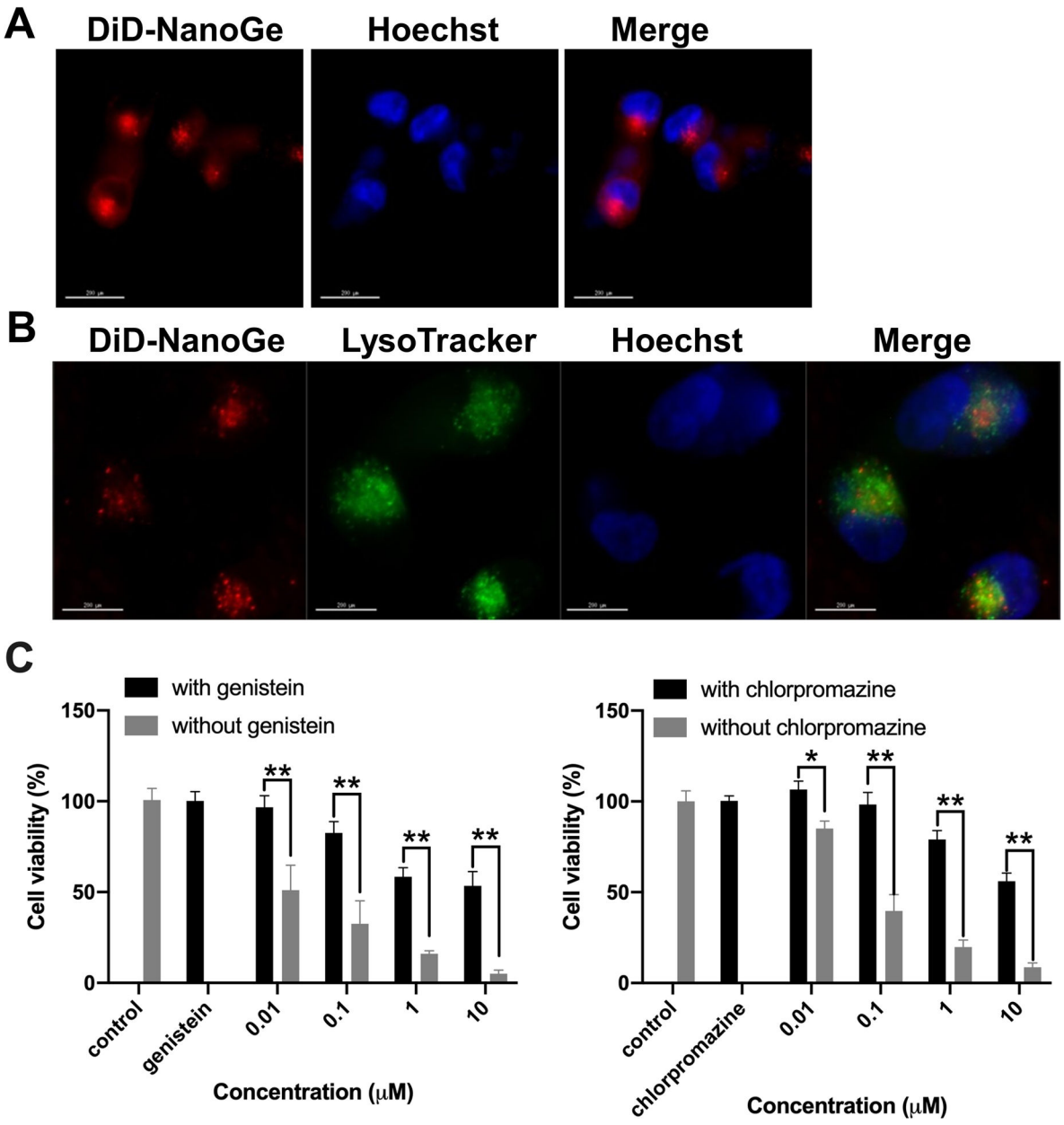

Fig 2.

NanoGe internalized cell via endocytotic pathways. (A) Confocal images showing the intracellular uptake of DiD-labeled NanoGe in PC-3M cells after 4h of incubation. (blue: Hoechst 33342 for nuclei). (B) The subcellular distribution of NanoGe was investigated by confocal microscopy (green: LysoTracker) (C) Cytotoxicity of NanoGe mediated by genistein and chlorpromazine was measured by the MTS method. NanoGe was internalized by PC-3M cells mainly through caveolae- and clathrin-mediated endocytotic pathways. *$P <$ 0.05, **$P < 0.01$.

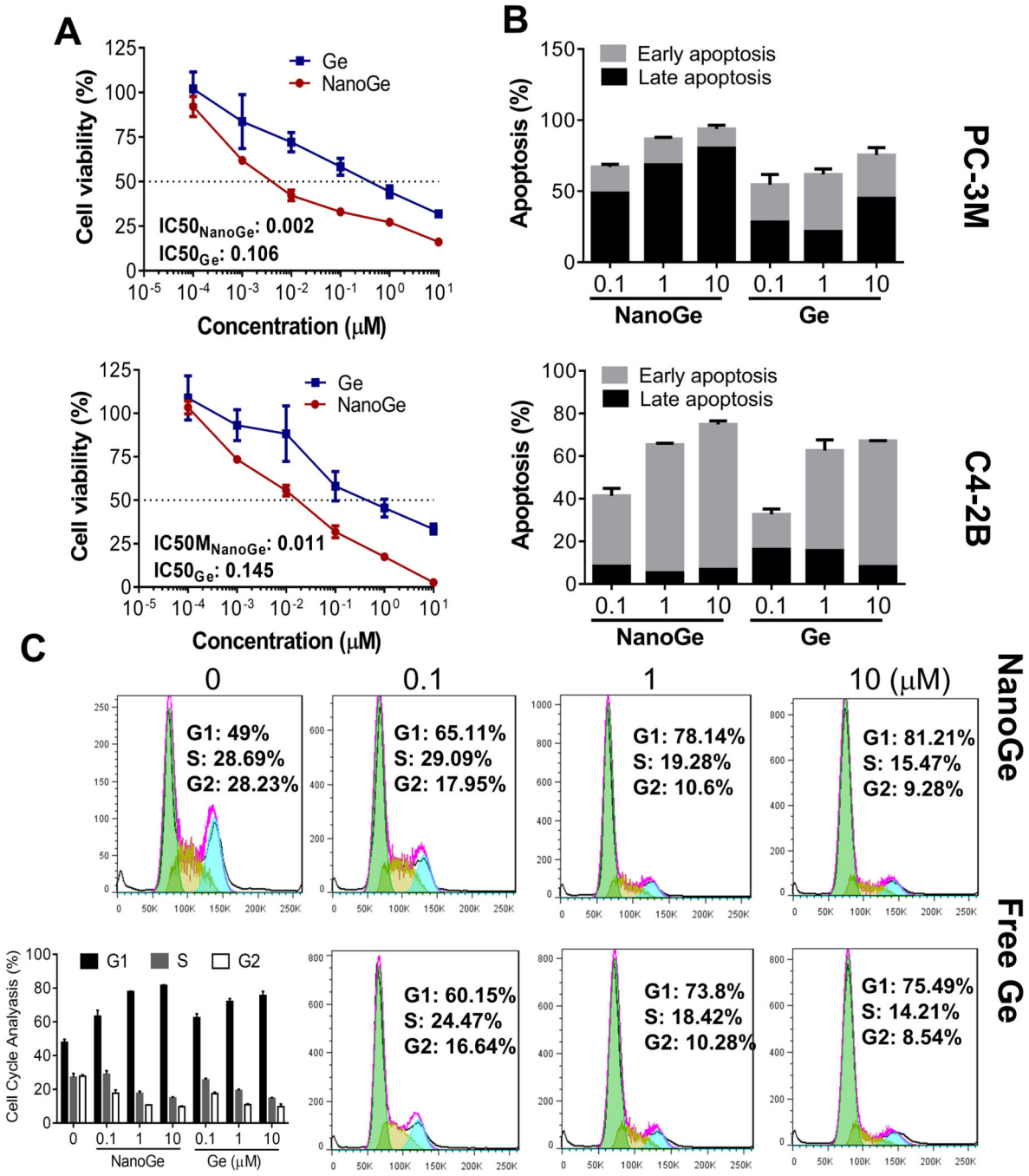

Fig 3.

NanoGe induced apoptosis of PC-3M and C4–2B prostate cancer cells. (A) The viability of prostate cancer cells after treatment with NanoGe (10^{-5} to 10 μM) for 48 h. (B) Flow cytometric analysis of apoptosis by Annexin V/PI dual staining assay after Ge and NanoGe treatment (0.1 to 10 μM) for 24 h. Annexin V+/PI− cells were considered as early apoptotic cells, while Annexin V+/PI+ cells were considered as late apoptotic cells. A dose-dependent apoptotic effect was observed after both treatments. (C) Cells were treated with NanoGe and

Ge for 24 h. Cell cycle progression was analyzed by flow cytometry. Ge induced G1 cell cycle arrest, while NanoGe further enhanced this effect.

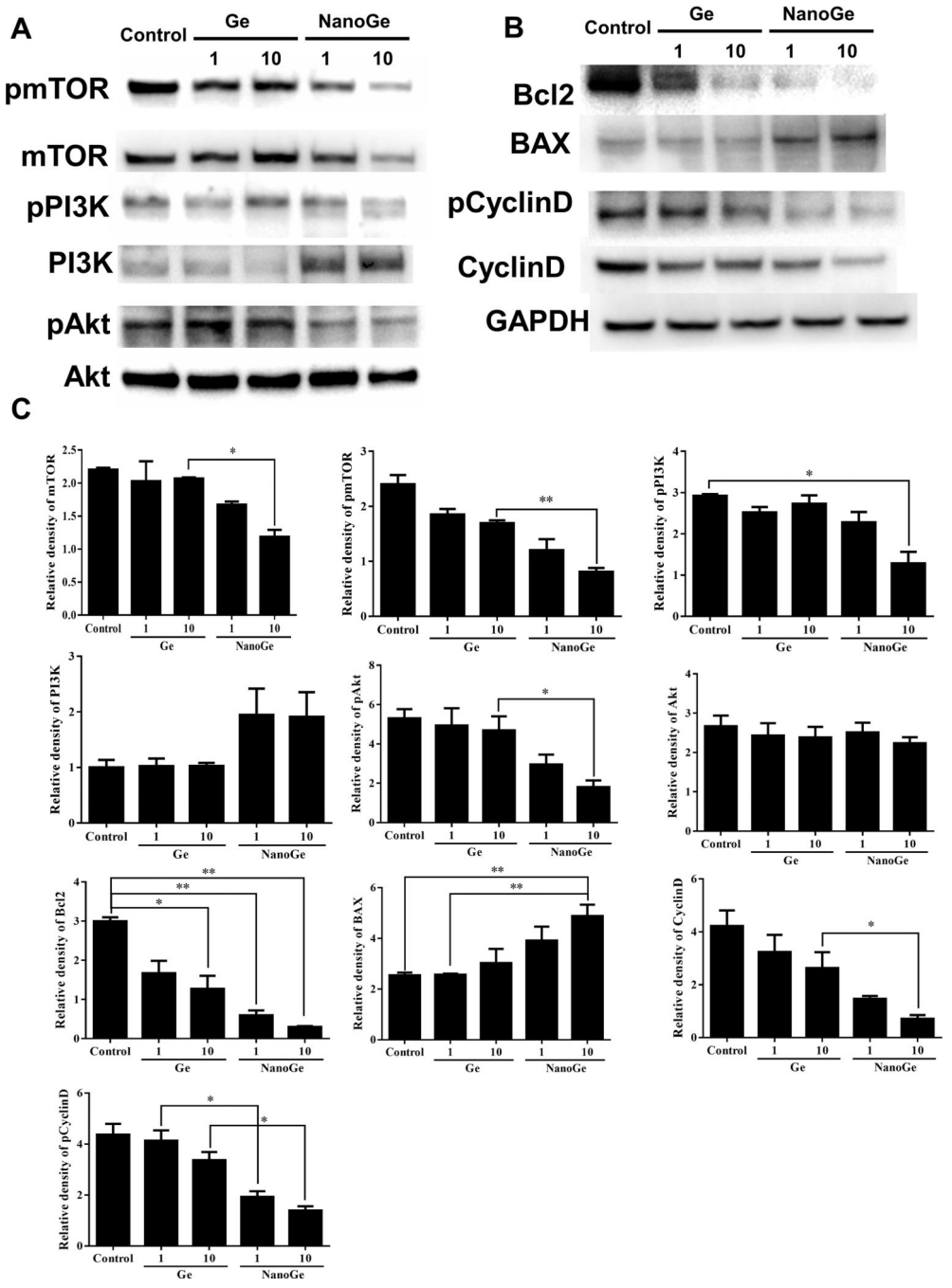

Fig 4.

The expression of the proteins related to the PI3K/mTOR pathway, apoptosis, and cell cycle regulation was analyzed by western blotting. Total cellular protein was extracted from PC-3M cells after 6 h treatment with different concentrations of free gedatolisib (1 and 10 μM) and NanoGe (1 and 10 μM gedatolisib). (A) Changes in the expression levels of p-mTOR, mTOR, p-PI3K, PI3K, p-Akt, and Akt after free gedatolisib and NanoGe treatment. (B) Western blot analysis of Bcl-2, Bax, cyclin D, and p-cyclin D expression after NanoGe

and gedatolisib treatment for 6 h. GAPDH was used as the loading control. (C) Quantitative analysis of western blotting results. *$P < 0.05$, **$P < 0.01$.

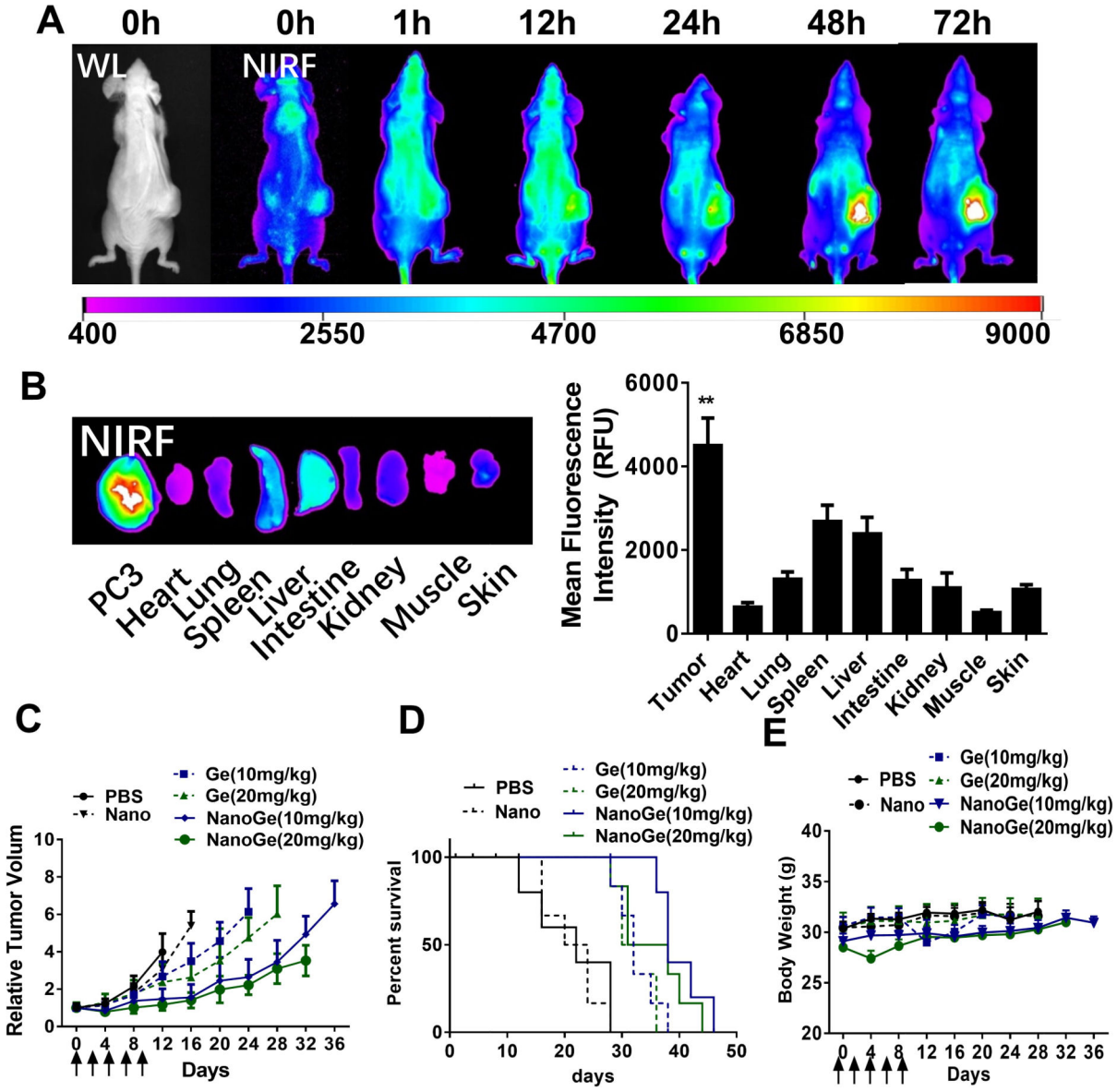

Fig 5.

In vivo therapeutic efficacy study of NanoGe in a PC-3M xenograft mouse model. (A) *In vivo* NIRF optical imaging of PC-3M xenograft mice after intravenous injection of DiD-labeled NanoGe was performed at different time points as indicated (24 h). (B) After the last time point (72 h), *ex vivo* NIRF images of dissected organs and tumors were obtained, and quantitative analysis was performed (n = 4). The relative changes in tumor volume (C), survival curve (D), and body weight (E) of mice bearing PC-3M tumors after treatment with PBS, blank DCM (Nano), free gedatolisib (10 and 20 mg/kg), and NanoGe (10 and 20 mg/kg gedatolisib) were measured every 4 days. All treatments were administrated via tail veins (black arrows). n = 6 per group. No significant difference was observed in changes in body weights between treatment groups. Tumors larger than 1000 mm^3 were considered as endpoint. Analysis was terminated once endpoint was reported in one mouse from each group.

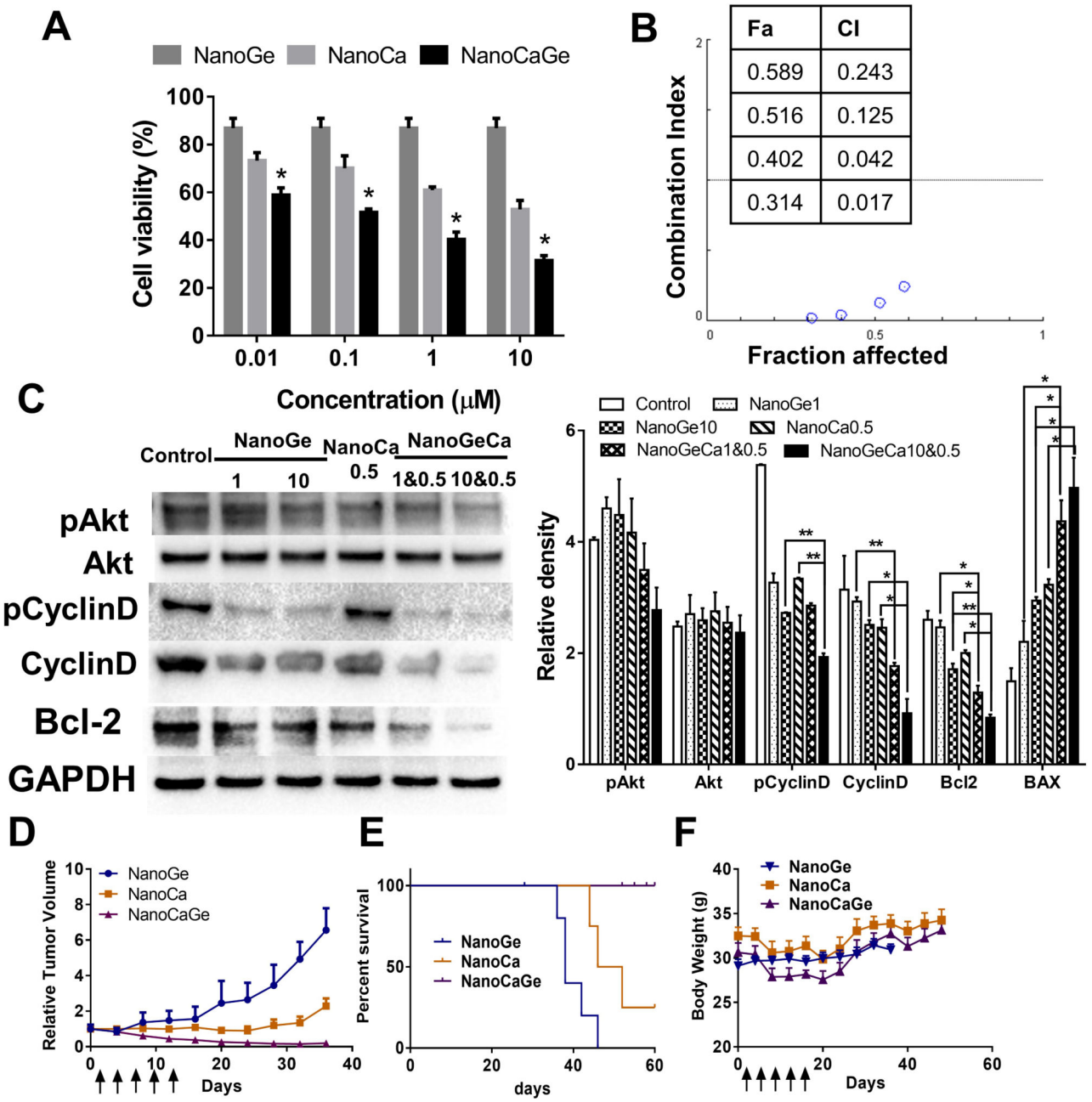

Fig 6.

In vitro and *in vivo* anticancer efficacy studies of NanoGe and NanoCa combination in a xenograft mouse model. (A) MTS assay for cell viability analysis after treatment with NanoGe (fixed at 10^{-4} μM gedatolisib) and NanoCa. NanoGe combined with different concentrations of NanoCa (0.01 to 10 μM Ca). (B) Combination index (CI) versus fraction affected (Fa) plot was calculated by CompuSyn and shown as combination effects (CI < 1 indicates synergism; CI = 1 indicates additive effect; CI > 1 indicates antagonism). (C) The effects of the combination treatment with NanoGe and NanoCa on p-Akt, Bcl-2, Bax, cyclin D, and p-cyclin D expression were analyzed by western blotting. Results were quantified using ImageJ. *$P < 0.05$, **$P < 0.01$. Relative changes in tumor volume (D), survival curve

(E), and body weight (F) of PC-3M tumor-bearing mice after treatment with NanoCa (10 mg/kg of cabazitaxel) and NanoCaGe (10 mg/kg of gedatolisib and 10 mg/kg of cabazitaxel) were measured every 4 days, as indicated by the arrows. Please note that we have also included tumors treated with 10 mg/kg of NanoGe (light blue, same group as Fig 5C–E) in this figure as control. n = 6 target lesions/group All treatments were administered via tail vein (black arrows). Tumors larger than 1000 mm^3 were considered as endpoint. Graph ended when one mouse in each group reached its endpoint.

Table1

Biochemistry panel of NSG mice treated with PBS, Ge, NanoGe, NanoCa, and NanoCaGe on the third day after the last treatment, (n = 3)

	ALT U/L	ASTU/L	BUN mg/dL	Creatinine mg/dL	Total Bilirubin mg/dL
PBS	64.8±5.10	264.05±21.65	32.60±0.40	0.17±0.07	0.08±0.01
Ge(10mg/kg)	47.6±7.73	219.97±32.71	20.97±1.39	0.10±0.01	0.10±0.01
Ge(20mg/kg)	25.57±0.99	83.30±4.48	22.00±1.46	0.11±0.02	0.09±0.01
NanoGe(10mg/kg)	43.77±7.92	181.03±23.56	26.33±0.88	0.17±0.03	0.10±0.01
NanoGe(20mg/kg)	39.13±0.19	174.50±5.63	27.37±0.43	0.09±0.01	0.09±0.01
DCM	24.47±1.73	59.10±2.55	19.63±0.96	0.11±0.01	0.09±0.02
NanoCa(10mg/kg)	40.05±1.84	91.30±34.51	16.10±0.23	0.12±0.02	0.10±0.02
NanoCaGe(10mg/kg&10mg/kg)	39.97±5.00	244.43±65.45	24.03±0.18	0.15±0.02	0.08±0.01

Table 2

Hematology profile of NSG mice treated with PBS, Ge, NanoGe, NanoCa, and NanoCaGe on thè third day after the last treatment. (n=3)

	WBC (K/ul)	RBC (M/ul)	Hemoglobin (g/dL)	Hematocrit %	Platelets (K/uL)
PBS	4.40±0.55	9.00±0.23	13.73±0.58	42.47±0.85	730.00±227.17
Ge(10mg/kg)	7.06±1.45	9.53±0.31	13.27±0.79	42.17±1.02	1053.33±70.10
Ge(20mg/kg)	5.20±0.35	8.76±0.41	12.77±0.62	38.23±1.21	1090.00±30.12
NanoGe(10mg/kg)	5.99±1.18	9.35±0.07	14.30±0.31	44.27±2.77	877.67±107.64
NanoGe(20mg/kg)	4.67±1.08	8.10±0.82	11.93±1.32	36.50±3.84	901.33±108.06
DCM	10.59±0.72	8.62±0.21	12.57±0.18	39.77±2.72	1018.67±112.80
NanoCa (10mg/kg)	4.20±1.56	7.76±0.28	11.90±1.49	34.53±1.44	1980.33±245.06
NanoCaGe(10mg/kg&10mg/kg)	7.85±3.13	7.17±0.25	11.40±0.31	33.13±0.54	2198.67±172.28